Highlights of Spanish Astrophysics XII, Proceedings of the XVI Scientific Meeting of the Spanish Astronomical Society held on July 15 - 19, 2024, in Granada, Spain. M. Manteiga, F. González Galindo, A. Labiano Ortega, M. Martínez González, N. Rea, M. Romero Gómez, A. Ulla Miguel, G. Yepes, C. Rodríguez López, A. Gómez García and C. Dafonte (eds.), 2025

New insights on the ionized gas phase of NGC 7319 with optical MEGARA/GTC data

Bellocchi, E.[1,2], Pereira-Santaella, M.[3], Gil de Paz, A.[1,2], Alonso-Herrero, A.[4], Garcia Burillo, S. [5], García Bernete, I. [6], Hoenig, S. [7] and GATOS collaboration

[1] Departmento de Física de la Tierra y Astrofísica, Fac. de CC Físicas, Universidad Complutense de Madrid, E-28040 Madrid, Spain
[2] Instituto de Física de Partículas y del Cosmos IPARCOS, Fac. de CC Físicas, Universidad Complutense de Madrid, E-28040 Madrid, Spain
[3] Instituto de Física Fundamental (IFF), CSIC, Serrano 123, 28006 Madrid, Spain
[4] Centro de Astrobiología (CAB), CSIC-INTA, Camino Bajo del Castillo s/n, 28692 Villanueva de la Cañada, Madrid, Spain
[5] Observatorio Astronómico Nacional (OAN-IGN)-Observatorio de Madrid, Alfonso XII, 3, 28014 Madrid, Spain
[6] Department of Physics, University of Oxford, Keble Road, Oxford OX1 3RH, UK
[7] School of Physics & Astronomy, University of Southampton, Hampshire, SO17 1BJ Southampton, UK

Abstract

According to numerical models, feedback from accreting supermassive black holes plays a central role in the evolution of galaxies. Kinetic feedback (or radio/jet-mode) is the most important form of AGN feedback in low accretion rate AGNs (i.e., the majority of AGN) and, therefore, it has a major impact on the evolution of most galaxies. Stephan's Quintet was targeted by JWST Early Release Observations and JWST/MIRI mid-IR spectroscopy was obtained for NGC 7319, the largest spiral in the group, which hosts a type 2 Seyfert AGN with a low-power radio jet. The JWST data analysis reveals a clear jet-ISM interaction, which is decelerating the relativistic jet and producing strong hot/warm molecular H_2 emission. We present preliminary results obtained using MEGARA/GTC to characterize the kinematics and physical conditions of the ionized phase of this textbook example of a jet-ISM interaction. The study of optical emission lines in several bands covering several ionization states and sensitive to different physical conditions allows us to characterize the shocked regions, the so-called N2 and S2 spots previously found. A multi-component approach is taken to properly characterize the systemic and the ionized gas outflow components and to derive the velocity and the size of the outflow as well as its mass, momentum and kinetic energy.

1 Introduction

Feedback from accreting super massive black holes (SMBHs) is thought to play a central role in the evolution of galaxies (see [11]). Current cosmological simulations require feedback from active galactic nuclei (AGN) to bring together the mass function of the ΛCDM dark matter halos and the high end of the galaxy mass function triggers the migration from the blue- to the red-sequence of galaxies by quenching the formation of stars, and establish the $M_{\star}$-σ relation ([12]). AGN feedback comes in two flavors: (1) a radiative-mode during a luminous quasar phase with a high accretion rate; and (2) a kinetic mode (or radio/jet-mode) which takes place in AGN with low accretion rates (i.e., the majority of the AGN). In the latter, the kinetic feedback is produced by relativistic jets launched near the SMBH. These low-power jets remain for a long time trapped in the ISM around the AGN affecting large gas volumes, thus having a large impact on the nuclear regions of these galaxies ([20]). As a consequence, the kinetic feedback due to low-power jets in low-luminosity AGN, can be the main evolution driver for most of the galaxies during the major part of their lives. However, essential questions for understanding the AGN kinetic feedback are still open: (i) How is the jet energy transferred to the ISM and the ionized outflows launched?; and (ii) What are the physical conditions and main ionization mechanism (shocks associated with the expanding radio jet)?

2 Our target: NGC 7319

NGC 7319 is a local type 2 Seyfert ($L_{14-195\ keV} = 10^{43.8}$ erg s^{-1}; N_H=$10^{23.8}$ cm^{-2}; d=98 Mpc) which is part of the Stephan's Quintet. It hosts a low-power radio jet ($L_{1.4\ GHz}$=$10^{22.5}$ W Hz^{-1}) which is almost coplanar with the galaxy disk with two asymmetric radio hotspots, N2 and S2 (Fig. 1). The northern radio hotspot N2 is closer to the AGN than S2 because the jet is interacting with the gas present in a dust lane, which decelerates the relativistic jet ([13]). For this reason, N2 is the perfect place to study kinetic feedback effects due to the transfer of energy and momentum from the jet to the ISM. Recent JWST/MIRI MRS observations allowed us, for the first time, to isolate the ionized gas and hot/warm molecular phases at the jet-ISM interaction spot at 300 pc (FWHM=0.6") spatial scale. This galaxy also contains a ∼400 km s^{-1} blue-shifted ionized gas outflow detected in [OIII]λ5007 Å ([2]) and Hα ([15]) up to large distances from the nucleus (∼4 kpc; see Fig. 2) at low spectral and spatial resolutions (R∼2000 and ∼3", respectively). This outflow is co-spatial with the radio lobes, perpendicular to the stellar disk and its kinematics major axis is aligned with the core-hotspots axis.

Among the projects being carried out within the GATOS collaboration[1], we aim to characterize ionized gas outflows using data taken with the MEGARA instrument ([10]). This galaxy is included as one of the targets, as has already been done for NGC2110 ([14]) and NGC5506 ([7]). In NGC 2110, the radio jet played an important role in affecting the ionized gas kinematics. In this work, we trace the ionized gas emission from the outflow and shock waves at the jet-ISM interaction spot (N2) with higher spectral (R∼6000) and spatial

[1] `https://gatos.myportfolio.com/`

(FWHM$\sim$1$''$) resolutions than previously done by [2, 15].

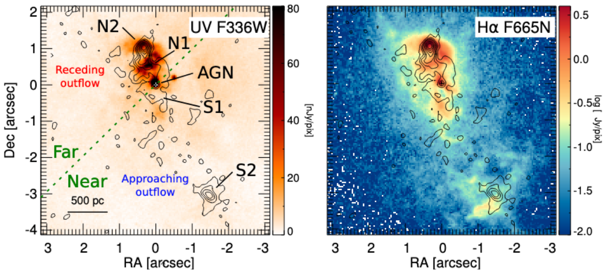

Figure 1: *Left:* Radio emission of the jet in NGC 7319. Overlay of the 1.4 GHz emission intensity contours on the near-UV/blue image (HST/WFC3 F336W; λ_p=0.335 μm). We indicate the location of the radio hotspots, N2 and S2, the nuclear diffuse radio lobes, N1 and S1, and the AGN. The jet-molecular gas interaction takes place at N2. *Right:* Hα emission from the continuum-subtracted HST/WFC3 F665N image. Figure taken from [13]. Scale of 0.448 kpc/$''$.

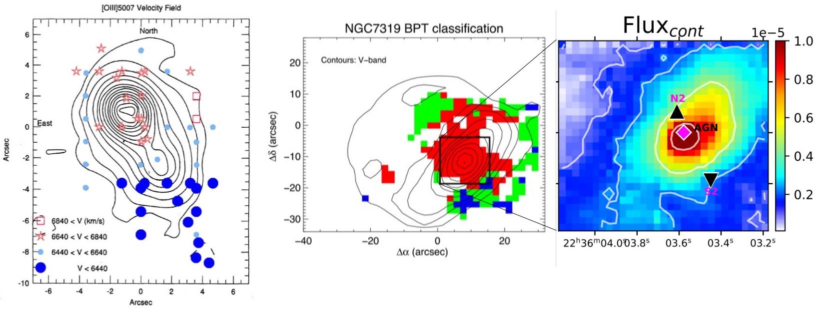

Figure 2: *Left:* [OIII]λ5007 velocity field (see [2]). *Middle:* BTP diagram from [15] using PPAK (2$''$ spaxel) based on [OIII]5007/Hβ vs. [NII]6584/Hα lines. Regions dominated by AGN emission are shown in red. The black square identifies the FoV covered by MEGARA-IFU (12.5$''$$\times$11.3$''$). *Right:* Continuum flux emission map from MEGARA-IFU (this work; resampled to a spaxel size of 0.4$''$). The continuum peak position identifies the AGN position (magenta diamond). The black (up and down) triangles identify the two radio hotspots, N2 and S2, respectively.

3 Data analysis

We derived the flux intensity and kinematic maps (velocity v, dispersion σ) for several ionized-gas emission lines, spanning multiple ionization states and sensitive to different physical conditions (e.g., Hγ+[OIII] λ4363, Hβ+[OIII] λ4959,5007, [NI]λ5200, [OI]λ6300,63, [SII]λ6717,30, [NII]λ6548,84+Hα, etc.). To this aim, the stellar emission was previously removed using pPXF ([5]), with stellar population synthesis models (SSP) from [18], based on the MILES stellar library (FWHM of 2.5 Å) and Padova+00 isochrones ([17]). After that, we applied a multi-component approach ([3]), fitting observed emission lines[2] like Hα and [OIII] lines of individual spectra with Gaussian profiles using an IDL routine (MPFITEXPR, implemented

[2]Line flux ratios and wavelengths are fixed according to atomic physics, with widths constrained to be equal for all lines and greater than the instrumental contribution.

by Craig Markwardt[3]). In particular, initial fits were performed with a single Gaussian profile (1 component, 1c) per line, adequate for most outer-region spectra. However, in inner regions, multi-component fits (2 or 3 components per line) were necessary. The multi-component fit allowed the identification of a systemic (narrow) and secondary (broad) component by width. When a third component was needed, it displayed the narrowest width.

To avoid overfitting, we considered the ϵ-criterion (see [6]) which compares the standard deviation of a continuum-free section (ϵ_{cont}) near the studied line with the residual standard deviation after fitting under the line of interest (ϵ_{line}). For the Hα+[NII] complex, residuals were derived from all three lines to address emission blending in some spaxels with broad profiles. For the [OIII] doublet, only the region under [OIII] λ5007 Å (the brightest line) was considered. We applied a threshold ratio of $\epsilon_{line}/\epsilon_{cont} \geq 1.5$ to justify adding components, a decision also supported by visual inspection, where asymmetric line profiles were often evident. This threshold prompted the addition of a secondary component (2c) and, in some cases, a third (3c), especially in regions aligned with the radio jet, after looking at the residuals in the 2c-fit case. For each emission line and component, we obtained central wavelength, width, and flux intensity, creating the kinematic maps shown in Fig. 3.

This analysis allows the derivation of outflow properties, such as velocity (v_{out}), size (R_{out}), mass, momentum, and kinetic energy.

4 Main results

4.1 Kinematic maps

As derived from the multi-component Gaussian fit of the Hα emission line, both the systemic and secondary components are observed across the entire field of view (FoV; $12.5'' \times 11.3''$ or $\sim$5.6×5.1 kpc^2), exhibiting complex and patchy distributions characterized by different kinematics. The third component is more compact than the secondary one and it is located in the direction of the radio jet. According to their widths (i.e., σ_{1c} = 100.3±19.1 km s^{-1}, σ_{2c} = 281.3±56.2 km s^{-1} and σ_{3c} = 66.6±8.4 km s^{-1}) and the velocity field patterns, the secondary and third components might be associated with the ionized outflow.

As shown in the Hα and [OIII] velocity fields of the systemic component (Fig. 3, 1c), a non-rotational pattern is apparent. Specifically, three filamentary (or horn-shaped) structures shown in the HST image (see Fig. 1, right) might reflect the complex kinematics observed in the norther part of the velocity field in both maps (i.e., N-S and NE-SW). These structures could be induced by the passage of the radio jet which might generate some turbulence in such regions. Specifically, in the [OIII] velocity dispersion maps of the systemic (1c) and broad (2c) components we found a clear σ-enhancement in the direction perpendicular to the radio jet. As found in [19], this could be explained as due to the interaction of the jet with ISM of the galaxy. The third component, located along the direction of the radio jet (with slightly varying orientations), shows the narrowest width and features two distinct regions in both Hα and [OIII] lines: a blue-shifted region towards the south and a red-shifted region towards the north. The difference in velocity with respect to the systemic (barycentric[4]) component

[3] `https://cow.physics.wisc.edu/~craigm/idl/idl.html`.

[4] We did not apply any correction for the heliocentric velocity, which is 23.0 km s^{-1}.

is significant, reaching up to ∼-600 km s^{-1} in the blue-shifted part, consistent with findings in [2] (∼-500 km s^{-1}). The distribution of the [OIII]λ5007 emission is more compact than that of Hα but it still exhibits similar kinematic properties as in Hα (see Fig. 3).

Our preliminary analysis seems to indicate that the second and third components are tracing a 3D ionized gas outflow with complex kinematics. The first component, on the other hand, seems to show the effects of the radio jet running through the galaxy based on the enhanced σ (similar to results for the MAGNUM survey; see [19]).

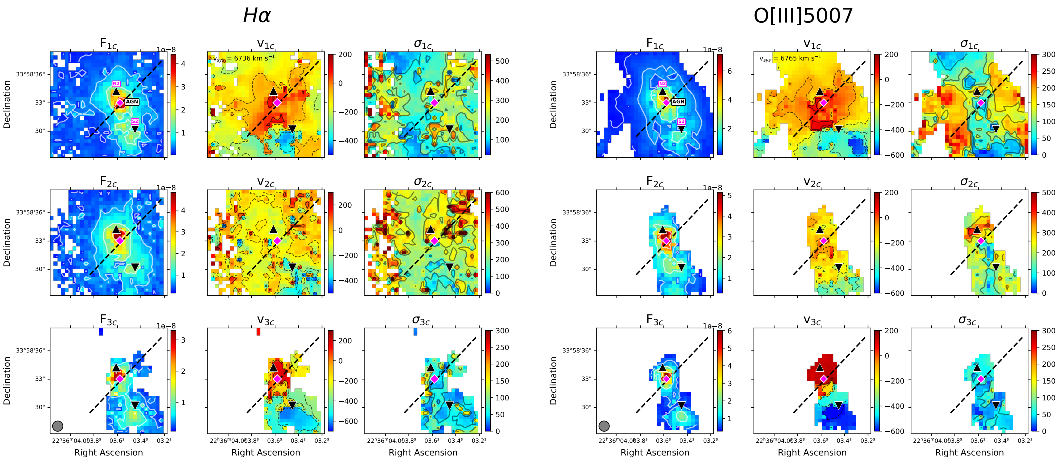

Figure 3: *From top to bottom. Left:* MEGARA Hα kinematic maps (flux intensity, velocity and velocity dispersion) for the systemic (1c), secondary-broad (2c) and third (3c) components. *Right:* Same as the Hα panels, but for the [OIII]λ5007 emission line. The black dashed line represents the position angle of the continuum emission (see Fig. 2). The derived (barycentric) systemic velocity is $v_{sys}\sim$ 6750 km s^{-1}. Symbols as in Fig 2. PSF FWHM (grey circle) is shown in the bottom left panel.

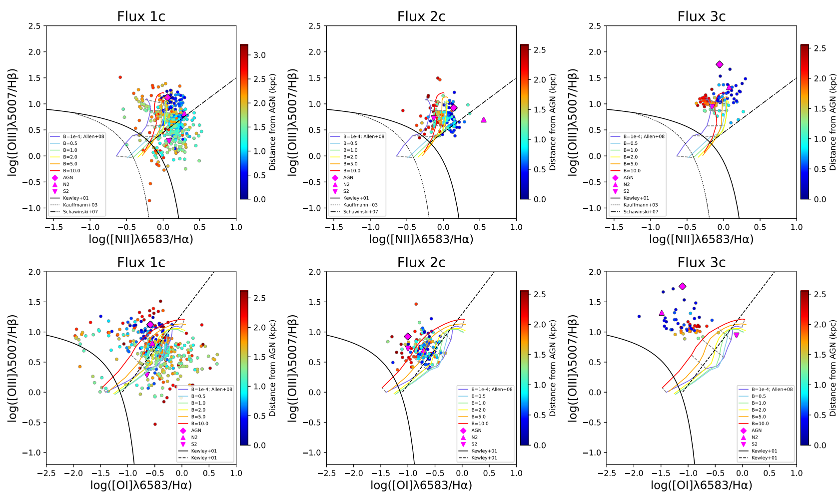

Figure 4: *Top:* N-BPT diagram derived for each individual components (1c, 2c, and 3c). *Bottom:* Same diagram as the N-BPT, but using the [OI] emission line (i.e., O-BPT diagram). Shock+precursor grid models from [1] are shown in all panels assuming $Z = Z_{\odot}$ and different values of the shock velocities (v = 200–1000 km s^{-1}) and magnetic field (B = 10^{-4}-10 μG).

4.2 BPT diagrams

Different spatially-resolved BPT diagrams were generated from our emission lines and compared with the photoionization grids produced by the Mappings III code ([1]) for fast radiative shocks. Specifically, the N-BPT and O-BPT diagrams are shown in Fig. 4. When adding the information about the distance of each point from the AGN, a clearer trend emerges. In particular, from the BPT diagrams, most of the data points of the 1c are found in the shock region and/or LINER region. Conversely, the 2c and 3c components appear to be more dominated by AGN photoionization with some contribution due to shocks.

5 Conclusions and Future work

Our preliminary analysis of NGC 7319 using MEGARA data reveals a highly complex ionized gas kinematics. The first component appears to reflect the impact of the radio jet traversing the galaxy, indicated by increased σ perpendicular to the jet direction, consistent with findings from the MAGNUM survey (see [19]). In contrast, the second and third components trace a 3D ionized gas outflow with intricate kinematics. This interpretation is further supported by the BPT diagrams, where the systemic component predominantly occupies the shock and/or LINER regions, while the 2c and 3c components are more AGN-photoionization dominated, with minimal shock influence. Future analyses will provide additional insights into the mechanisms driving these phenomena in NGC 7319.

Acknowledgments

EB and AGdP acknowledge support from the Spanish grants PID2022-138621NB-I00 and PID2021-123417OB-I00, funded by MCIN/AEI/10.13039/501100011033/FEDER, EU. AAH acknowledges support from PID2021-124665NB-I00 funded by MCIN/AEI/10.13039/501100011033 and by ERDF *A way of making Europe*.

References

[1] Allen M. G., Groves B. A., Dopita M. A., Sutherland R. S., Kewley L. J., 2008, ApJS, 178, 20
[2] Aoki, K., et al., 1996, AJ, 111, 140.
[3] Bellocchi, E., Arribas, S., Colina, L., & Miralles-Caballero, D. 2013, A&A, 557, A59
[4] Calzetti, D., Armus, L., Bohlin, R. C., et al. 2000, ApJ, 533, 682
[5] Cappellari M., Emsellem E., 2004, PASP, 116, 138
[6] Cazzoli, S., Hermosa Muñoz, L., Márquez, I., et al. 2022, A&A, 664, A135
[7] Esposito, F., Alonso-Herrero, A., García-Burillo, S., et al. 2024, A&A, 686, A46
[8] Fiore, F., Feruglio, C., Shankar, F., et al. 2017, A&A, 601, A143
[9] Fluetsch A. et al., 2021, MNRAS, 505, 5753
[10] Gil de Paz, A., Carrasco, E., Gallego, J., et al. 2018, Proc. SPIE, 10702
[11] Harrison, C. M., et al., 2018, Nature, 2, 198.
[12] Di Matteo, T., et al., 2005, Nature, 433, 604.
[13] Pereira-Santaella, M., Álvarez-Márquez, J., García-Bernete, I., et al. 2022, A&A, 665, L11
[14] Peralta de Arriba, L., et al., 2023, A&A, 675, A58
[15] Rodríguez- Baras, M., et al., 2014, MNRAS, 442, 495.
[16] Rupke, D. S., Veilleux, S., & Sanders, D. B. 2005, ApJS, 160, 87
[17] Sánchez-Blázquez, P., Peletier, R. F., Jiménez-Vicente, J., et al. 2006, MNRAS, 371, 703
[18] Vazdekis A., Sánchez-Bl ázquez P., Falcón-Barroso J., et al. 2010, MNRAS, 404, 1639
[19] Venturi, G., Cresci, G., Marconi, A., et al. 2021, A&A, 648, A17
[20] Villar Martín, M., Emonts, B. H. C., Cabrera Lavers, A., et al. 2021, A&A,650, A84
[21] Woo, J.-H., & Urry, C. M. 2002, ApJ, 579, 530